Materials Research Bulletin 44 (2009) 1738–1742

Contents lists available at ScienceDirect

Materials Research Bulletin

journal homepage: www.elsevier.com/locate/matresbu

Preparation and electrical properties of $x CaRuO_3/(1-x)CaTiO_3$ perovskite composites

Shuqiang Jiao *, Krishnankutty-Nair P. Kumar, Kamal Tripuraneni Kilby, Derek J. Fray

Department of Materials Science and Metallurgy, University of Cambridge, Pembroke Street, Cambridge CB2 3QZ, UK

ARTICLE INFO

Article history:
Received 27 January 2009
Received in revised form 17 March 2009
Accepted 26 March 2009
Available online 10 April 2009

Keywords:
A. Composites
A. Electronic materials
A. Nanostructure

ABSTRACT

$CaRuO_3$–$CaTiO_3$ ceramic composites were prepared by sintering for short times for potential applications in the areas of electronic ceramics. Scanning electron microscopy and energy dispersive X-ray analysis showed two separate phases, $CaRuO_3$ and $CaTiO_3$ in the composite. Conductivity data, measured by the four-probe method, showed that the composites have high electrical conductivity when $x \geq 0.19$ in $x CaRuO_3$–$(1-x)CaTiO_3$ composites. Furthermore, the nanoparticle of calcium ruthenate prepared by reverse micelle synthesis was used to be conductive agent for the composite. The result shows that the use of nano-sized calcium ruthenate enabled higher electrical conductivity to be maintained down to $x = 0.09$.

1. Introduction

Mixed oxides with perovskite ($CaTiO_3$) structure exhibit a wide variety of electrical and magnetic properties. Calcium ruthenate ($CaRuO_3$), a perovskite-type compound, is well known as an important conductive material [1–8], which shows low electrical conductivity (10 S cm^{-1}) at room temperature. Moreover, $CaRuO_3$ has no magnetic order; therefore, it could be an effective electrode material for ferroelectric devices [9,10] and for use in Josephson junctions as a metallic barrier [11,12]. However, at present $CaRuO_3$ is unlikely to be suitable for industrial applications due to relatively high cost. One of the commonly followed approaches to reducing cost is to make a composite with a relatively inexpensive second phase. However, sintering of mixtures of ruthenates and titanates results in a solid solution which, at low concentrations of ruthenate, have very low conductivities, 10^{-1} to 10^{-2} S cm^{-1} for $x = 0.3$ in $CaRu_xTi_{1-x}O_3$ [13] and 7×10^{-4} S cm^{-1} for $x = 0.1$ in $SrRu_xTi_{1-x}O_3$ at room temperature [14]. These low values make the materials unsuitable for use in electronic devices. In this work, a method is described which allows the high conductivity to be maintained at low concentrations of the calcium ruthenate.

2. Experimental

2.1. Preparation of $xCaRuO_3/(1-x)CaTiO_3$ composites

$CaRuO_3$ powders were prepared by the standard solid reaction technique. 99.95% pure $CaCO_3$ (10996, Alfa Aesar) and RuO_2 (40336, Alfa Aesar) were mixed using mortar and pestle in stoichiometric proportion. The mixture was then placed into an alumina crucible and heated to 950 °C for 2–12 h. $CaTiO_3$ powders were prepared using the same approach from $CaCO_3$ and TiO_2 as starting materials with a selected reaction temperature of 1400 °C. To prepare the desired perovskite $x CaRuO_3/(1-x)CaTiO_3$ composites, the $CaRuO_3$ and $CaTiO_3$ powders were thoroughly mixed together with arbitrarily selected ratios, where $x = 0.11$, 0.19, 0.28, 0.41, and 0.69. The mixtures were individually pressed into pellets with 20 mm diameter and 3 mm thickness using a uniaxial pressure of 1.6 tons cm^{-2}. The pellets were then sintered at 1400 °C for 2–12 h.

2.2. Preparation of nano-sized calcium ruthenate

The reverse micelle system was used to prepared nano-sized calcium ruthenate. Ruthenium(III) chloride hydrate ($RuCl_3$ XH_2O, and calcium chloride dehydrate ($CaCl_2$ $2H_2O$, Alfa Awsar: 99.9%) were used as starting materials to prepare the nano-precursor, and sodium carbonate (Na_2CO_3, Fisher Scientific: 99.5%) was used as the precipitating agent. All solutions were prepared with double distilled water. The micelle system consisted of *n*-octane (Alfa Awsar: 99%) as continuous oil phase, cetyltrimethylammonium bromide (CTAB, Alfa Awsar: 99%) as the surfactant, 1-butanol (Alfa

* Corresponding author. Tel.: +44 1223334315; fax: +44 1223335637.
E-mail addresses: sj332@cam.ac.uk, sqjiao_ustb@yahoo.com.cn (S. Jiao), djf25@cam.ac.uk (D.J. Fray).

0025-5408/$ – see front matter © 2009 Elsevier Ltd. All rights reserved.
doi:10.1016/j.materresbull.2009.03.019

Awsar: 99%) as the cosurfactant, and an aqueous solution as the dispersion phase. A solution was prepared by dissolving 1.260 g of $RuCl_3$ XH_2O and 0.736 g of $CaCl_2$ $2H_2O$ in 20 ml of double distilled water. This solution was dispersed in a mixture of 80 ml of *n*-octane, 15 ml of 1-butanol and 16 g of CTAB to form a micelle. Another micelle of similar composition was prepared using the Na_2CO_3 solution which dissolving 1.6 g of Na_2CO_3 in 20 ml of double distilled water. These two micelles were mixed using a magnetic stirrer for 1 h. The black precipitate that formed was extracted by centrifuging at 2000 rpm for 15 min. The precipitate was then washed by ethanol three times by centrifuging process. The product after washing was dried at 100 °C. The dried powders were calcinated in separated batches at different temperature for 2–8 h.

2.3. Preparation of nano-sized $CaRuO_3$/$CaTiO_3$ composites

The $CaRuO_3$ nano-precursor and $CaTiO_3$ powders were thoroughly mixed together with the selected ratios. The mixtures were individually pressed into pellets with 20 mm diameter and 3 mm thickness using a uniaxial pressure of 1.6 tons cm^{-2}. The pellets were then sintered at 1400 °C for 2–12 h.

2.4. Physical characterization

X-ray diffraction (XRD), field-emission SEM and TEM were used for characterization of the products. The electric conductivity of the composite pellets was measured by four-probe approach.

3. Results and discussion

For the standard solid-state reactions, the samples as prepared have been analyzed by the X-ray diffraction technique. Fig. 1 presents the XRD patterns of as prepared $CaRuO_3$ and $CaTiO_3$ by solid-state reaction $CaCO_3$ and corresponding oxides with a long sintering time of 12 h. All peaks visible in this figure pertain to well-crystallized orthorhombic structures of $CaRuO_3$ and $CaTiO_3$. Only negligible amounts of the raw material phase could be observed in the diffraction traces. However, the obvious amounts of raw materials are still remaining when the sintered period is less than 8 h.

This work is focused on the electrical properties of the $x CaRuO_3/(1-x)CaTiO_3$ composites. To measure the conductivity of the composites, it is necessary to make the composite pellets with low porosity by optimising sintering conditions. The pellets of the $x CaRuO_3/(1-x)CaTiO_3$ composites were sintered at 1400 °C with different durations of 2–12 h. The composite pellets as prepared have been characterized, and the results showed that the pellets with low porosity would be prepared after a long sintering period of 12 h.

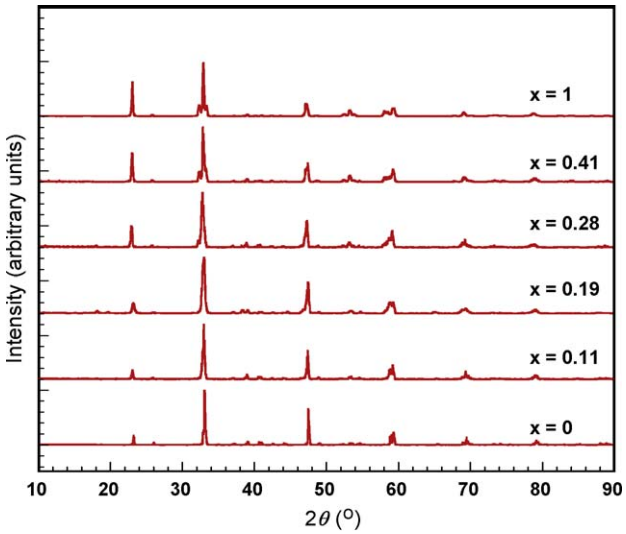

Fig. 2. XRD patterns of composite pellets with different ratio of x (from 0 to 1).

The XRD patterns of the prepared $x CaRuO_3/(1-x)CaTiO_3$ composites are shown in Fig. 2, where $x = 0.11$, 0.19, 0.28, 0.41, and 0.69. The XRD patterns of pure $CaRuO_3$ and $CaTiO_3$ perovskites sintered at 1400 °C are also shown. It is noticeable from Fig. 2 that the XRD patterns of the composite materials are similar to the pure perovskite materials. However, upon further inspection it is evident that as x increases the XRD pattern of the composite progressively correspond more to the $CaRuO_3$ diffractogram. Fig. 3 highlights this difference, when x is greater than 0.41, the peaks relating to $CaRuO_3$ (2 0 0) and (0 0 2) appear instead of $CaTiO_3$ (0 2 0) and (2 0 0).

The sintered pellets including pure $CaRuO_3$ and $CaTiO_3$ were analyzed by scanning electron microscopy (SEM, JEOL 5500). The results are shown in Fig. 4. Fig. 4a and d shows the morphologies of $CaRuO_3$ and $CaTiO_3$ pellets sintered at 1400 °C. It is observable that the $CaTiO_3$ grain size is larger and that the pellet is less porous

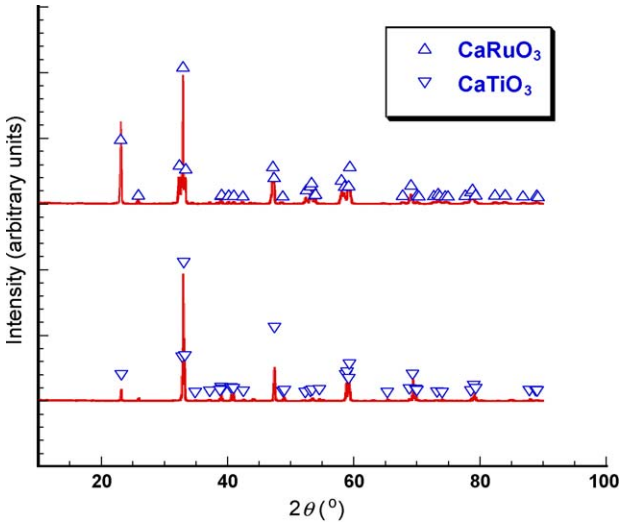

Fig. 1. XRD patterns of $CaRuO_3$ and $CaTiO_3$ prepared.

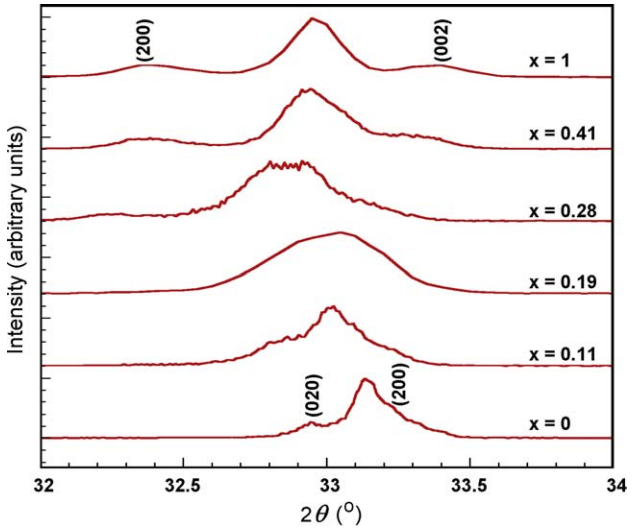

Fig. 3. Detailed XRD patterns of composite pellets.

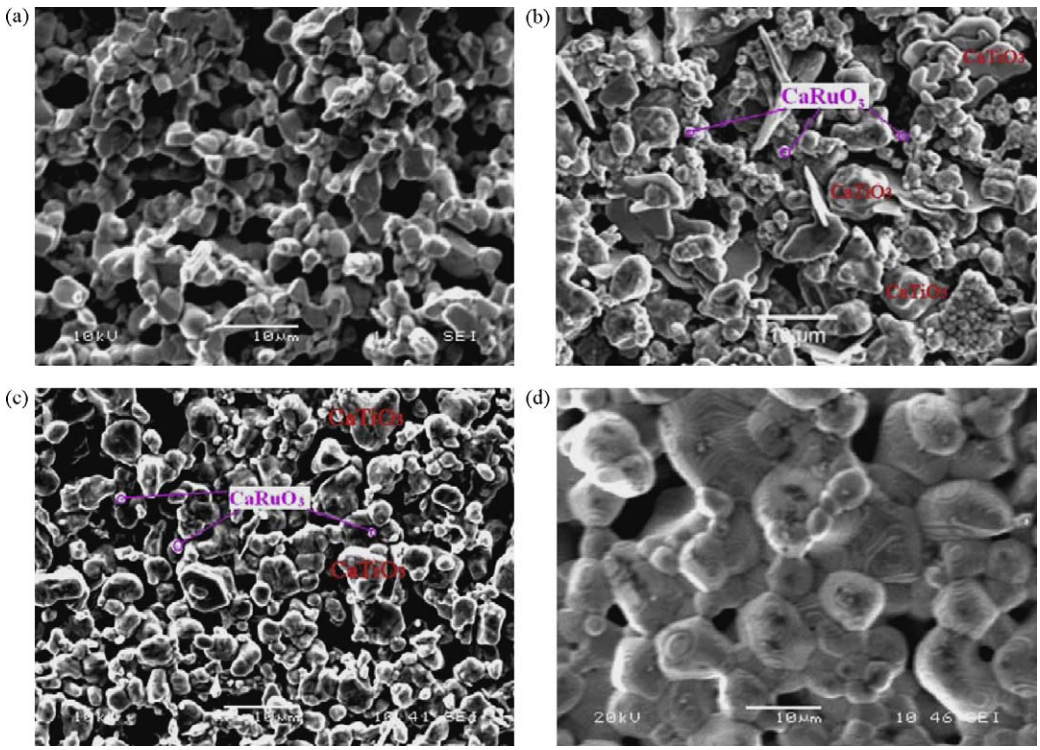

Fig. 4. SEM images of $CaRuO_3$ (a), $CaTiO_3$ pellets (d), composite pellets with the ratio of $x = 0.19$ (b) and $x = 0.11$ (c).

when compared to $CaRuO_3$. Fig. 4b and c presents the morphologies of the composite materials with a ratio of $x = 0.19$ and 0.11, respectively. It is clear that the sizes of the composite grains are smaller than that of pure $CaTiO_3$. To evaluate the phase constitution associated with its microstructure, energy dispersive X-ray analysis (EDX) had been used. Generally, results show that there are separate phases in the composite mixture. The bigger grains are primarily comprised of elements Ca, Ti, and O, suggesting a $CaTiO_3$ rich phase. Conversely, EDX analysis conducted on smaller particles indicates the presence of a $CaRuO_3$ rich phase.

Moreover, it is interesting to observe that the composite with the ratio of $x = 0.28$ showed particles with a unique plate-like morphology and is shown in Fig. 5. The plate-like particles are homogenously distributed in the composite matrix. Fig. 4b also showed few plate-like particles, but not as much as Fig. 5. EDX analysis elucidates that this phase primarily consists of Ca, Ru, and O, indicating the possibility of the formation of a Ru rich phase under certain conditions. At this point it is not possible to pinpoint the exact conditions or the composition.

It was aforementioned that the specific cost of a $CaRuO_3$/$CaTiO_3$ composite material will be significantly lower than pure $CaRuO_3$, hence ensuring a greater economic feasibility for this material to be used in industrial applications. However, it is important that the composites should exhibit low electrical resistivity for the projected electrode applications. A four-probe method was used to measure the electrical resistivity of the composite materials. A plot of electrical resistivity versus the $CaRuO_3$ component composition is shown in Fig. 6. It is noticeable that the relationship between electrical resistivity and $CaRuO_3$ content is not linear. The electrical resistivity increases rapidly

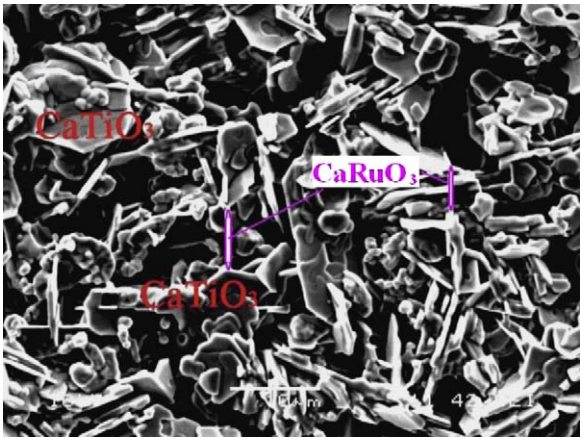

Fig. 5. SEM image of composite pellets with the ratio of $x = 0.28$.

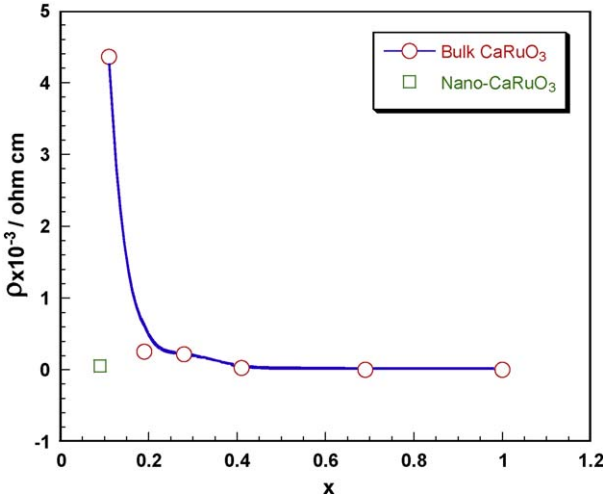

Fig. 6. The change in electrical resistivity for composite pellets consisting of varying amounts of the $CaRuO_3$ component.

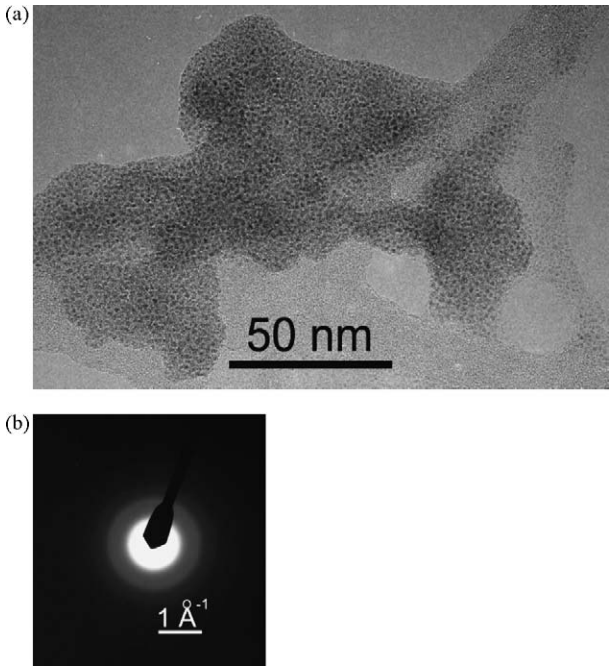

Fig. 7. TEM image (a) and the selected area electron diffraction pattern (b) of the Ca–Ru–O precursor prepared in reverse micelle.

when the composite ratio of x is less than 0.19. Therefore, despite the high porosity of all of the tested pellets, composite materials with $x \geq 0.19$ have an electrical conductivity that is high enough for applications as electrode materials.

It is known that when one powder is dispersed in another, the properties that result are influenced by the particle size ration and volume fraction [15]. In order to maximise the conductivity and to minimise the amount of calcium ruthenate in the composite, it was decided to use a $CaRuO_3$ nano-precursor. This again was prepared by the reverse micelle synthesis. The morphology of the dried precursor was observed through TEM analysis, with the relevant micrographs presented in Fig. 7a. It was found in Fig. 7b that the precursor consisted of an amorphous structure for its particles. The average diameter of the amorphous Ca–Ru–O particles, measured from several TEM micrographs, was shown to be around 5 nm (within a range of ±2 nm). The lack of contrast was associated to their amorphous structure.

Fig. 8a shows the XRD pattern of the powder sintered the precursor at 850 °C. It is evident that all of peaks are corresponding to the $CaRuO_3$. From TEM image shown in Fig. 8b, it is seen that they were growing with one direction and formed nanorods.

Hereinbefore, the electrical resistivity would be affected by the size of powders. We aimed to prepare the composite of 0.09nano-$CaRuO_3$/0.91$CaTiO_3$. The $CaRuO_3$ nano-precursor and $CaTiO_3$ powders were thoroughly mixed together with the selected ratios. The mixtures were individually pressed into pellets with 20 mm diameter and 3 mm thickness using a uniaxial pressure of 1.6 tons cm^{-2}. The pellets were then sintered at 1400 °C for 2–12 h. Indeed, the pellets as prepared with short sintering time show the high porosity. The sintering time was increased to make dense pellet. The pellets sintered in the duration of 12 h were analyzed by scanning electron microscopy. The results are shown in Fig. 9. It is observable that the $CaTiO_3$ grain size is larger and that the pellet is less porous when compared to bulk $CaRuO_3$. To evaluate the phase constitution associated with its microstructure, energy dispersive X-ray analysis had been used. Generally, results show that there are separate phases in the composite mixture. The bigger grains are primarily comprised of elements Ca, Ti, and O,

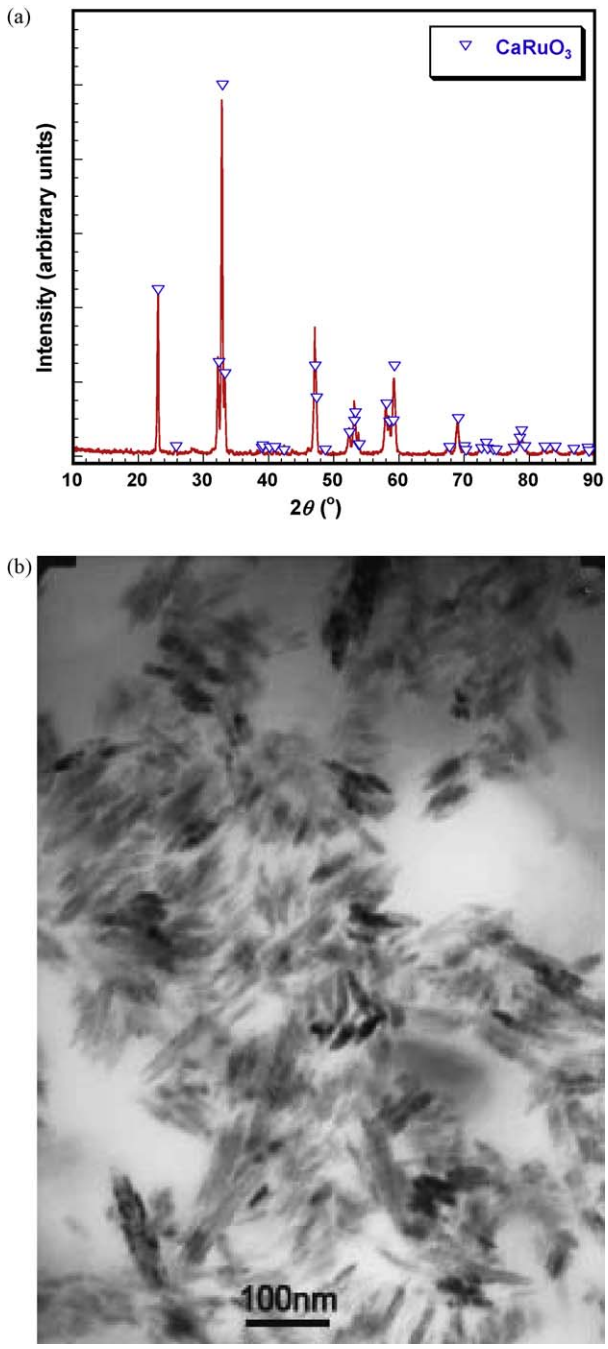

Fig. 8. TEM image (a) and XRD spectrum (b) of the $CaRuO_3$ prepared by sintering the precursor at 850 °C for 2 h.

suggesting a $CaTiO_3$ rich phase (+1). Conversely, EDX analysis conducted on smaller particles indicates the presence of a $CaRuO_3$ rich phase (+2).

A four-probe method was used to measure the electrical resistivity of the composite pellet of 0.09nano-$CaRuO_3$/0.91$CaTiO_3$. The corresponding result, compared to the plot of electrical resistivity versus the bulk $CaRuO_3$ component composition mentioned before which is shown in Fig. 6. It is noticeable that the electrical resistivity of the pellet is much lower than that of the same composite ratio when the bulk $CaRuO_3$ used. Therefore, the composite pellet with $x = 0.09$ nano-$CaRuO_3$ has an electrical resistivity that is low enough for applications as electrode materials.

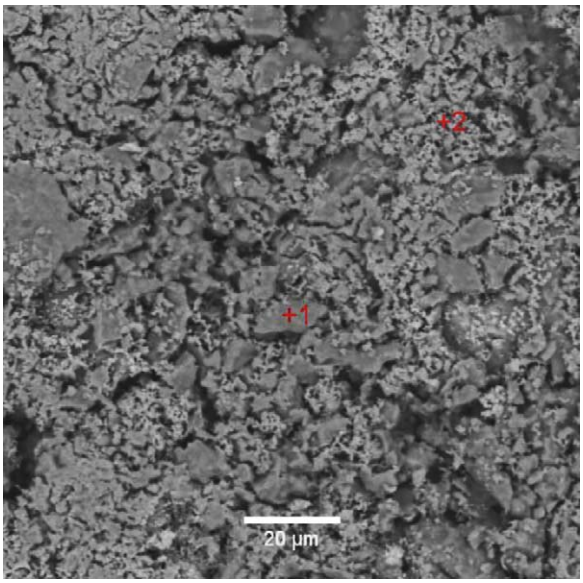

Fig. 9. SEM image of the composite pellet prepared by nano-$CaRuO_3$ and $CaTiO_3$.

4. Conclusions

Mixed composites of $CaRuO_3$ and $CaTiO_3$ have been investigated which are prepared at high temperature but are stable at room temperature. By the use of nano-particulate $CaRuO_3$ high electrical conductivities were obtained down to $x = 0.09$ in $CaRu_xTi_{1-x}O_3$. This can be compared with a solid solution, which is obtained by sintering for long periods, of the two materials where the conductivities were orders.

Acknowledgement

The authors are grateful to the Engineering and Physical Sciences Research Council (EPSRC) for financial support.

References

[1] R.J. Bouchard, J.L. Gillson, Mater. Res. Bull. 7 (1972) 873.
[2] J.B. Wiley, K.R. Poeppelmeier, Mater. Res. Bull. 26 (1991) 1201.
[3] H. Kobayashi, M. Nagata, R. Kanno, Y. Kawamoto, Mater. Res. Bull. 29 (1994) 1271.
[4] N. Higashi, N. Okuda, H. Funakubo, Jpn. J. Appl. Phys. 39 (2000) 2780.
[5] A. Banerjee, R. Prasad, V. Venugopal, J. Alloy Compd. 358 (2003) 321.
[6] M.V. Rama Rao, V.G. Sathe, D. Sornadurai, B. Panidrahi, T. Shripathi, J. Phys. Chem. 62 (2001) 797.
[7] W. Bensch, H.W. Schmalle, A. Reller, Solid State Ionics 43 (1990) 171.
[8] C. Mallika, O.M. Sreedharan, J. Alloy Compd. 177 (1991) 273.
[9] H. Funakubo, T. Oikawa, N. Higashi, K. Saito, J. Cryst. Growth 235 (2002) 401.
[10] T. Wu, D. Tsai, Mater. Chem. Phys. 85 (2004) 88.
[11] K. Char, M.S. Colclough, T.H. Geballe, K.E. Myers, Appl. Phys. Lett. 62 (1993) 196.
[12] S.G. Lee, K. Park, Y.K. Park, J.C. Park, Appl. Phys. Lett. 64 (1994) 2028.
[13] T. He, R.J. Cava, Phys. Rev. B 63 (2001) 172403.
[14] S.L. Cuffini, V.A. Macagno, R.E. Carbonio, A. Melo, E. trolland, J.L. Gautier, J. Solid State Chem. 105 (1993) 161.
[15] R.P. Kusy, J. Appl. Phys. 48 (1977) 5301.